International Journal of Biological Macromolecules 206 (2022) 553–566

Contents lists available at ScienceDirect

International Journal of Biological Macromolecules

journal homepage: www.elsevier.com/locate/ijbiomac

Efficient extraction of carrageenans from *Chondrus crispus* for the green synthesis of gold nanoparticles and formulation of printable hydrogels

Milena Álvarez-Viñas [a], Noelia González-Ballesteros [b], M. Dolores Torres [a], Lucía López-Hortas [a], Candida Vanini [c], Guido Domingo [c], M. Carmen Rodríguez-Argüelles [b], Herminia Domínguez [a,*]

[a] CINBIO, Facultade de Ciencias (Campus Ourense), Universidade de Vigo, Edificio Politécnico, As Lagoas, 32004 Ourense, Spain
[b] CINBIO, Universidade de Vigo, Departamento de Química Inorgánica, 36310 Vigo, Spain
[c] Department of Biotechnology and Life Sciences, University of Insubria, via J. Hdunant 3, 21100 Varese, Italy

A B S T R A C T

The integral utilization of sustainable resources with versatile, efficient and cleaner processes is encouraged. Hydrothermal treatment with subcritical water is a chemical free, tunable and rapid technology providing enhanced yield compared to conventional extraction and was explored for the benign by design extraction and depolymerization of carrageenan from *Chondrus crispus*. Up to 90% of the seaweed was solubilized operating under nonisothermal regime during heating up to 200 °C and 75.5% crude carrageenan yield was attained at 140 °C. Crude carrageenan could not be precipitated by ethanol from the extracts produced at 180 °C and higher temperatures, but ultrafiltration (100 kDa) of the extract obtained at 160 °C provided comparable recovery yields and similar rheological features to those of the ethanol precipitated product. Operation at 140 °C was preferred based on the higher recovery yield of the biopolymer and the whole extract was suitable for the green synthesis of polycrystalline decahedral quasi-spherical gold nanoparticles with a mean size distribution of 8.4 nm and Z potential value of −40.2 mV. Alternatively, the crude carrageen fraction was used for the formulation of printable biopolymer based gels with suitable mechanical properties, including a relevant gel strength enhancement (about 10-fold) when compared with conventional procedures.

1. Introduction

Marine macroalgae biomass has been mostly used as food or destined to produce hydrocolloids, but offers great potential for the generation of both energy and valuable bioproducts. Particularly interesting is the use of greener solvents and efficient environmentally friendly processes [1,2] following a biorefinery scheme for the integral valorization of this widely available and renewable resource [2,4]. Hydrothermal treatment with subcritical water as solvent has been proposed as a key stage for the biorefinery of brown seaweeds providing higher yields than conventional extraction, or extraction assisted by ultrasound and/or enzymes [5,6]. This is regarded as a green tunable technology more rapid than conventional, requiring no chemicals and less grinding of the raw material [7]. In addition, further depolymerization can be attained, an effect that could be desirable when the biological properties of the polymers are closely dependent on the molecular weight.

Carrageenans are linear sulfated polysaccharides found in red seaweeds, approved for food applications with gelling, stabilizing and thickening functions. The different types of carrageenan have distinctive gelling abilities and the hybrid carrageenans exhibit unique characteristics intermediate among those of different pure carrageenan types [8]. *Chondrus crispus* is an example of an underutilized genus synthesizing different types of carrageenans [9]. Applications in pharmaceutics, and cosmetics, particularly for its antiviral, immunomodulatory, anticoagulant, antioxidant, and antitumoral properties are emerging [10]. These properties are closely dependent on the carrageenan type and structure, which can be determined by the selected extraction and processing methods [11]. Conventional extraction of these hydrocolloids is based on alkaline extraction [12] and recent trends are focused on the use of intensification processes and greener solvents [4,5].

Hydrocolloids offer nutritional, functional and bioactive potential as a food ingredient, but also as controlled release excipients for nutraceuticals or drug systems for biomedical applications [13]. Carrageenans can be available at low cost, being nontoxic, renewable and biocompatible, show promising properties for tissue engineering, regenerative medicine and drug delivery formulations, an area receiving increased attention for food, nutraceutical and pharmaceutical applications to enhance the stability and availability of bioactives [14–16].

Gold nanoparticles are currently the subject of extensive research due to their interesting physical, chemical and biological features, making them suitable for their use in several areas, such as in the energy and environmental sectors, food industry and in medicine [17,18].

* Corresponding author.
E-mail address: herminia@uvigo.es (H. Domínguez).

https://doi.org/10.1016/j.ijbiomac.2022.02.145
Received 14 January 2022; Received in revised form 17 February 2022; Accepted 24 February 2022
Available online 1 March 2022

However, the use of nanomaterials in food industry and medicine are still limited due to the traditional methods of synthesis, that employ toxic solvents or reagents potentially increasing the toxicity of the nanomaterials. Aiming to overcome this drawback, researchers are focusing in alternative methods of synthesis, employing natural and biocompatible compounds eliminating the use of toxic reagents [19]. In this regard, carrageenan extracted from other carrageenophyte species was used for the synthesis of gold nanoparticles with enhanced antioxidant and antitumoral activity [20].

Bioprinting is a versatile tool for regenerative medicine that can be done in three dimensions (3D), and further advances rely on the development of adequate bio-inks with satisfactory printability, biocompatibility and mechanical integrity [21]. Biopolymers from marine sources offer these advantages and are abundant and biologically active compared to other polymers from different sources. Carrageenan can be used to generate *in situ* 3D printed gel materials valid for food and pharmaceutical applications, without needing chemical additives or initiators [21,22].

Subcritical water extraction provided higher carrageenan yields from the seaweeds than conventional solvents [5] and allowed the extraction of additional product from the residual solids after conventional carrageenan extraction [23]. Therefore, the present study aims at the efficient extraction with subcritical water of both gelling fractions from *C. crispus* and the evaluation of selected products for rheological properties and for their potential for incorporation in two model encapsulation systems: green synthesis of Au nanoparticles and 3D printing.

2. Materials and methods

2.1. Materials

Chondrus crispus (9.6 ± 0.3 g/100 g of moisture content) was kindly supplied by Compañía Española de Algas Marinas S.A., CEAMSA (Pontevedra, Spain). All samples were stored at room temperature in airtight plastic bags in the dark until analysis.

2.2. Conventional alkaline extraction

Carrageenan was extracted following the previously reported conventional procedure [24]. *Chondrus crispus* ground to powder size was used and 1.5 g were immersed in an alkaline KOH solution of 0.1 M concentration (50 mL) at 80 °C and for 2 h. The suspensions were cooled to 40 °C with distilled water (50 mL), and the pH was adjusted to 8–9 with HCl to stop the alkaline action during the extraction process.

2.3. Hydrothermal extraction with subcritical water

Samples of seaweed were combined with distilled water at a ratio of 30:1 (*w*/w), placed in a pressurised Parr Instruments reactor (series 4842, USA) and heated until the selected temperature in the range of 120–200 °C, requiring times in the range 10–60 min, corresponding to severity values (log R0) in the range 1.36–3.90. The severity factor log R_0 is defined based on Eq. 1 [25]:

$$R_0 = t \cdot exp\left[\frac{T-100}{14.75}\right] \quad (1)$$

where t is the reaction time (min) and T is temperature (°C). Once reached the target temperature, the reactor was cooled down in order to separate by filtration both solid and liquid phases. The carrageenan in the liquid phase was recovered by precipitation adding ethanol (96%) using an ethanol:liquid ratio 1.5:1 (v/v) [24]. After vacuum filtration the crude carrageenan was ethanol washed twice, dried (40 °C), milled to 200 μm average particle size previously to be stored in closed containers at room temperature until further study. Depending on the composition of the extracts under the tested conditions, different processing stages were further proposed (Fig. 1).

2.4. Ultrasound assisted depolymerisation

Liquid phases obtained after autohydrolysis treatment were incubated in threaded jars using an ultrasonic bath with thermal control (±3 °C) (FB 11207, Fisherbrand, Germany). The operation conditions were selected based on those previously optimized for other seaweeds [26], frequency (80 kHz), temperature (25 °C), time (90 min), power (3100 W) working in sweep mode. Samples were freeze-dried before further analysis. Those containing the highest carrageenan yields (140 °C) were deeper assessed by antiproliferative tests.

2.5. Membrane fractionation

The extracts obtained from the hydrothermal treatments at 160 °C and at 200 °C were processed in a sequence of ultrafiltration membranes in decreasing cut-off order from 100 to 1 kDa (Merk-Millipore, Germany). Each retentate was collected and analysed and the corresponding permeates were processed in the next membrane, all operating in concentration mode to a final volume concentration ratio (VCR) of 7.

2.6. Microwave hydrodiffusion and gravity treatment

In order to test the possibility of processing the whole wet seaweed, an innovative drying technology was also tested, based on microwave heating and gravity drainage of the water naturally present in seaweed, named microwave hydrodiffusion and gravity (MHG). The MHG treatment was tried on seaweed rehydrated at room temperature (liquid/solid ratio ~500 v/w) for 60 min. Rehydrated seaweeds (~100 g) were placed in toroidal geometry in a NEOS-GR MA126 equipment (Milestone Srl, Italy) using 800 W for 2 min and 400 W for 2 min. The solid phase was cooled at room temperature for 30 min to prevent burning, and the sample was rotated before a final stage at 100 W for 30 min. These processing conditions were previously optimized (unpublished work). The recovered fractions (1 mL) of liquid phases were mixed and stored at 4 °C in the light absence until their analysis. All experiments were performed at least in duplicate.

2.7. Gelled matrices formulation

Hybrid carrageenan extracted by hydrothermal treatment of *C. crispus* at selected temperatures (120, 140 and 160 °C) was used as gelling agent for the development of a number of gelled matrices. A first set of hybrid carrageenan-based gelled matrices was prepared at fixed biopolymer content (1%, *w*/w) and ionic strength (KCl or $CaCl_2$, 0.1 M) using water as solvent following the procedure reported elsewhere [8]. A second set of gelled matrices was formulated (KCl 0.1 M, 1%) based on the results obtained after rheological testing of the first set, using as solvent the liquid extract of hydrothermal treatment with the optimal antioxidant features (200 °C) or the recovered MHG liquid extracts. A third set of hybrid carrageenan gels (KCl_120, 0.1 M, 1%) was made using as solvent the permeates or retentates from hydrothermal extracts (160 and 200 °C) after fractionation in ultrafiltration membranes. To achieve a comprehensive use of the seaweed, a fourth set of hybrid carrageenan gelled matrices (KCl 120, 0.1 M, 1%), incorporated with the recovered solids (RS) after hydrothermal treatment (10%, *w*/w), was formulated using water as solvent. To extend the potential applications, one last set of gels at the same gelling conditions was proposed including selected nanoparticles (2%, w/w). For all gelled matrices sets, the corresponding amount of solid samples was dispersed in the selected solvent and heated up to 80 °C for 30 min with constant stirring as previously reported [27]. Hot solutions were directly used for further 3D printing trials, whereas formulated gelled matrices were cold stored for 24 h before rheological testing in order to ensure full gels maturation.

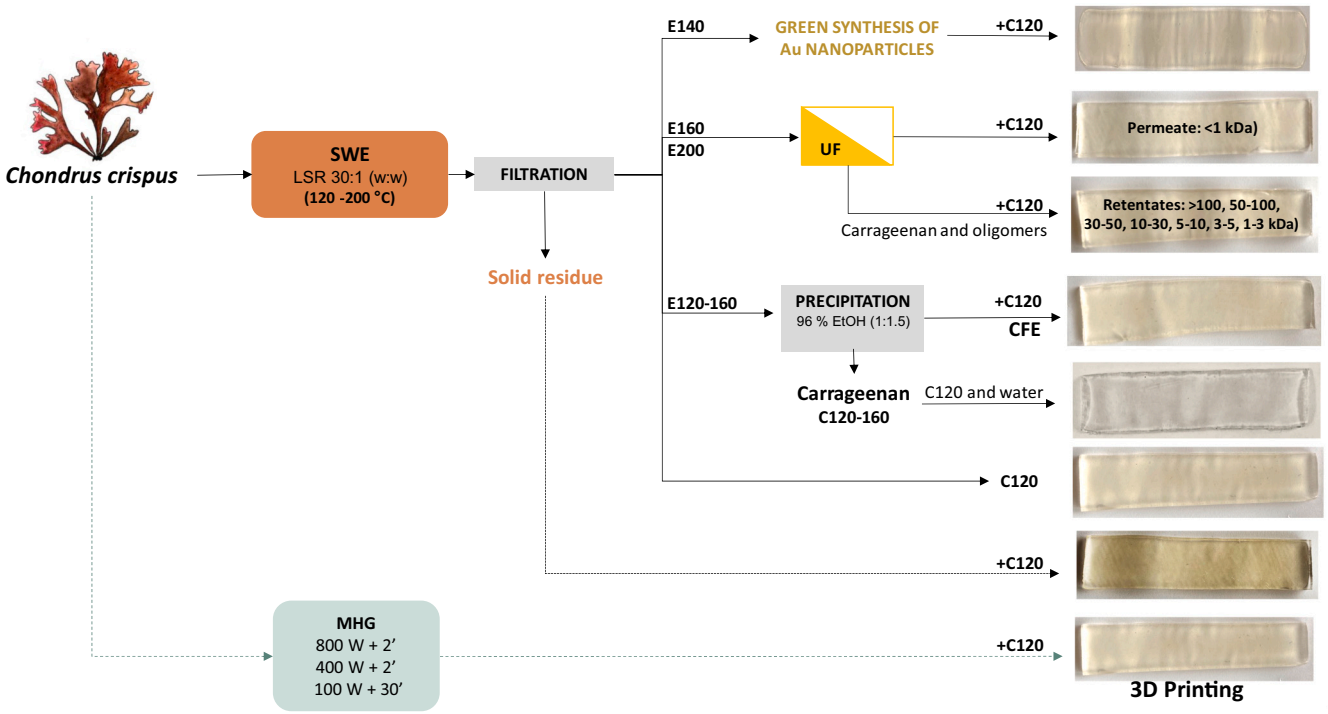

Fig. 1. Flow diagram of the process studied for the hydrothermal processing of *Chondrus crispus*. SWE: subcritical water extraction or hydrothermal treatment; MHG: microwave hydrodiffusion and gravity; CFE: carrageenan free extract.

Note here that 3D prints were also stored in the fridge (4 °C) after printing processing during the same period of time before further testing.

2.8. 3D printing

3D printing tests of above systems were conducted on a Foodini 3D printer (Natural Machines, Barcelona, Spain). The printed model for this work was designed with a rectangular shape (80 × 20 × 2 mm) using Foodini creator software. The above hot carrageenan solutions feed were dosed using a syringe extruder with 0.8 mm nozzle and gellified *in situ* during the 3D printing process. The printing settings were directly assigned as a new material using as the main parameters, the printing speed (1200 mm/min), ingredient flow (0.8), gap between layers (2 mm) and heating temperature (70 °C). Note here that preliminary trials were made to define the optimal printing conditions based on the final rheological properties of the final prints and following the recommendations given in a previous study working with commercial κ-carrageenan [22]. All measurements were carried out at least in triplicate.

2.9. Synthesis of gold nanoparticles

Chondrus crispus freeze-dried extract obtained by hydrothermal treatment at 140 °C was selected for the preparation of gold nanoparticles (AuNP). The freeze-dried extract was dissolved in milli-Q water at a concentration of 0.25 mg/mL. Then, different volumes of and aqueous solution 0.01 M of $HAuCl_4$ were added to the aqueous extract under continuous stirring. The most favourable reaction conditions were found out after several assays performed modifying the concentration of the extract solution (ranging from 0.5 mg/mL to 0.04 mg/mL) and $HAuCl_4$ employed (concentrations ranged from 0.16 to 0.41 mM), pH and temperature.

2.10. Analytical methodology

2.10.1. Chemical characterization

Moisture and ash content were gravimetrically determined at 105 °C and at 575 °C, respectively. Total nitrogen was determined by Kjeldahl and the value was converted to protein using the factor 4.92, specific for red seaweed [28]. Soluble protein was quantified by incubating samples with the Bradford reagent (Sigma, Spain) and incubated for 5 min at room temperature. The absorbance was measured at 595 nm and compared to a standard curve prepared with bovine serum albumin (BSA) (Sigma, Spain). Mineral content was measured after digestion of ashes in microwave Marsxpress (CEM, USA) with HNO_3 and H_2O_2 at 1600 W for 15 min and 200 °C for 10 min. The content of Na and K was determined by Atomic Emission Spectrophotometry (AES), Zn, Ca, Mg, Fe, and Cu were determined by Atomic Absorption Spectrophotometry (AAS) using a 220 Fast Sequential Spectrophotometer (Varian, CA) and Cd and Pb by Inductively Coupled Plasma Mass Spectrometry (ICP-MS) (X Series, Thermo Scientific, USA).

Sulfate content was measured using a method based on ionic chromatography (Metrohm Advanced IC-861, Switzerland) fitted with a Metrosep A Supp 5-250 column (250 × 4 mm) and equipped with an IC-819 detector, using as mobile phase 3.2 mM sodium carbonate/1 mM sodium bicarbonate (0.70 mL/min) [29]. All above measurements were performed at least in triplicate. The soluble sulphate content was determined by the gelatin-barium chloride method [30] after samples were hydrolysed by trichloroacetic acid (4%) (Sigma-Aldrich, Spain). The gelatin-$BaCl_2$ previously prepared reagent was added and mixed using a vortex, and after 15 min at room temperature, the absorbance was measured at 500 nm.

Total phenolic content was determined by mixing samples with the Folin-Ciocalteau reagent (1 N) and sodium carbonate at 20%, and incubation in darkness at room temperature for 45 min. The absorbance was measured at 730 nm using distilled water as blank and the standard curve was prepared with gallic acid (Sigma, Spain).

Saccharide composition of the oligomeric soluble fraction in the liquid phases was analysed after a posthydrolysis step. The generated

liquid phase, once filtered through 0.45 μm membranes was analysed by high performed liquid chromatography (1100 series, Agilent, Germany) using an Aminex HPX-87H (300 × 7.8 mm, BioRad, Hercules, CA, USA) column operating at 60 °C with 0.003 M H_2SO_4 at 0.6 mL/min as mobile phase.

2.10.2. Fourier-Transform Infrared Spectroscopy (FTIR)

The dried crude carrageenan samples obtained were lyophilised (Christ Alpha 2-4 LD plus, Germany), blended with KBr and analysed by FTIR (Nicolet 6700) fitted with a detector DTGS KBr, and the software used was OMNIC. The spectra of the samples were achieved over the range selected from 500 to 1500 nm (spectral resolution: 4 cm^{-1} and 32 scans min^{-1}). The AuNPs dispersion was fully dried in an oven at 80 °C and the residue obtained was pulverized and used for the preparation of the KBr pellet before analysis in a Jasco FT/IR-6100 spectrophotometer (JASCO, Tokyo, Japan) in a wavelength range from 4000 to 400 cm^{-1}. The samples were tested at least in duplicate.

2.10.3. High Performance Size Exclusion Chromatography

The molar mass distribution of the extracts, membrane fractions and crude carrageenan obtained under the studied temperature conditions were evaluated by High Performance Size Exclusion Chromatography (HPSEC). An arrangement of two columns in series (6 × 150 mm TSKGel SuperMultipore PW-H from Tosoh Bioscience, Germany) fitted by a TSKGel guardcolumn SuperMP(PW)-H (4.6 × 35 mm) and a refractive index detector was used. The mobile phase used was Milli-Q water at 0.6 mL/min. Poly (ethylene oxide) with different molecular weight ($2.36{\cdot}10^4$–$7.86{\cdot}10^5$ g/mol) (Tosoh Bioscience, Japan) were used as standards.

2.10.4. Proteins and peptides isolation and purification

Freeze dried *C. crispus* extracts from hydrothermal treatments were resuspended in water. Proteins were precipitated overnight at −20 °C using 1:5 volume of 0.1 M ammonium acetate in methanol. The supernatant, containing peptides and other compounds, was removed by centrifuging at 15.000 g for 15 min. The remaining precipitate was further washed twice with 0.1 ammonium acetate solution and once with pre-cooled 80% acetone. Each washing phase included 20 min centrifugation at 15000 *g*. The pellets containing proteins, were finally resuspended in 100 μL of FASP SDS-lysis buffer (SDS 20% *w*/w, 0,25 M Tris/HCl pH 7.5, DTT 100 mM). Precipitated proteins were quantified by the 2-D Quant-kit (GE Healthcare).

Peptides contained in the supernatants were purified using Amicon® Ultra-0.5 Centrifugal Filter Devices to remove proteins with a molecular weight above 30 kDa. Samples were further purified and concentrated using the SPE Clean-up Kit (provided by Waters). This last step allowed to obtain highly purified and concentrated samples suitable for subsequent MS-HPLC analysis.

2.10.4.1. MS-HPLC analyses. Protein samples were trypsin digested by using FASP (Filter Aided Sample Preparation) method [31].

Free peptides and the extracted tryptic fragments generated from precipitated proteins were analysed using a gel- and label- free approach. MS/MS analyzes were performed after reverse phase separation of peptides (Liquid Chromatography–Electro Spray Tandem Mass Spectrometry, LC–ESI-MS/MS). Chromatography separations were conducted on ACQUITY UPLC Peptide BEH C18 Column (300 Å, 1.7 μm, 2.1 mm × 150 mm) using a linear gradient from 2% to 70% ACN 0.1% formic acid with a flow of 100 μL/min. Total run lasted 120 min. Acquisitions were performed in the data-dependent MS/MS scanning mode (full MS scan range of 140–2000 *m/z* followed by Zoom scan for the most intense ion from the MS scan and full MS/MS for the most intense ion from the zoom scan). Because of the poor *Chondrus crispus* database found, peptides and proteins identifications were conducted by correlation of uninterpreted tandem mass spectra to the entries of a protein database of Rhodophyta using Bioworks software. Only proteins with a minimum probability of $1{\cdot}10^{-3}$ were considered.

2.10.4.2. SDS-PAGE. Sodium dodecyl sulfate–polyacrylamide gel electrophoresis (SDS-PAGE) of the protein fraction obtained after extraction of *C. crispus* hydrothermal extracts was carried out according to standard protocols (He, 2011). Briefly, 30 μg protein of each sample were mixed with the loading buffer (50 mM Tris-HCl, pH 6.8, 2% (w/v) SDS (w/v), 10% glycerol (v/v), and 0.01% (w/v) bromophenol blue) and then loaded onto a 12% polyacrylamide gel. The electrophoresis was conducted at a constant voltage of 120 *V*. After electrophoresis, the gel was stained with 0.25% (w/v) Coomassie Blue R-250 in 8% (v/v) acetic acid and 46% (v/v) ethanol for 30 min and subsequently detained with a solution containing 10% (v/v) acetic acid and 30% (v/v) ethanol. A molecular-weight protein marker (*Perfect Protein™ Markers*, 10–225 kDa; Merck Millipore, Darmstadt, Germany) was used to estimate the mass of the protein bands.

2.10.5. Rheological behavior

Small amplitude oscillatory shear (SAOS) measurements were carried out at least in triplicate on the formulated hybrid carrageenan gelled matrices and the corresponding prepared by 3D printing using a MCR302 controlled-stress rheometer (Anton Paar Physica, Austria). A sand blasted plate-plate geometry (2 mm gap, 25 mm diameter) was used to monitor the viscoelastic behavior, in terms of elastic modulus (G′) and viscous modulus (G″), of the systems at 25 °C. Above samples were carefully loaded on the measuring system, sealed with light paraffin oil to avoid water evaporation and left to rest for 5 min to allow temperature and structural equilibration. Then, stress sweeps were run at fixed frequencies (0.1 and 10 Hz) to limit the linear viscoelastic region (< 42 Pa) at tested temperature. Afterwards, frequency sweeps at 10 Pa from 0.1 to 10 Hz were conducted to determine the viscoelastic behavior of the gelled matrices providing a fingerprint-like profile of the matured gel.

2.10.6. Antioxidant properties

Reducing power was determined as the reduction of Fe^{3+} to Fe^{2+} [32]. One mL of sample was mixed with 2.5 mL phosphate buffer and 2.5 mL of potassium ferricyanide (1%) and the mixture was incubated at 50 °C for 30 min. After the addition of 2.5 mL of trichloroacetic acid (10%) and centrifugation, the supernatant was mixed with the same volume of distilled water and half of 0.1% ferric chloride. Absorbance was read at 700 nm against a standard curve prepared with ascorbic acid.

The ABTS [2,2-azinobis(3-ethyl-benzothiazoline-6-sulfonate)] radical cation ($ABTS^{\cdot+}$) scavenging was determined as previously reported [33]. The absorbance was measured at 734 nm after an incubation of samples in the diluted $ABTS^{\cdot+}$ solution for 6 min and values were expressed was expressed as TEAC value (Trolox Equivalent Antioxidant Capacity).

The α,α–Diphenyl-β-picrylhydrazyl (DPPH) radical scavenging was evaluated as previously reported [34]. The inhibition was expressed as the percentual reduction in absorbance readings at 515 nm. All the assays were performed at least in triplicate.

2.10.7. Antiproliferative activity

The cytotoxic activity of extracts and Au nanoparticles was initially evaluated in different human carcinoma cell lines (A549, A2780, HT-29, Hela 229) at 0.1 mg/mL, and when possible, lower concentrations were tested to estimate IC_{50} values. Cisplatinum was used as a control. A2780 cells were cultivated on RPMI 1640, A549 cells on Dulbeco Modified Eagle's Medium-low glucose, Hela 229 cells on Dulbeco Modified Eagle's Medium and HT-29 cells were cultivated on McCoy's 5A Medium. All systems were supplemented with 10% Fetal Bovine Serum (10%, FBS, Sigma) in a controlled air atmosphere (95% air/5% CO_2, 37 °C). The cell

growth inhibition was measured by MTT (3-[4,5-dimethylthiazol-2-yl]-2,-5 diphenyltretrazolium bromid, Sigma) analysis with 10,000 cells/well. The extracts dissolved in Milli-Q water were incorporated and incubated (95% air/5% CO2) at 37 °C for 72 h. The MTT (10 μL) was added and the mixture was incubated for 4 h followed by the addition of sodium dodecyl sulfate (100 μL, SDS) and incubation for 14 h before reading absorbance at 595 nm (Tecan Infinite M1000 Pro, Austria) and the results were expressed as growth inhibition (%).

2.10.8. Gold nanoparticles characterization

Ultraviolet-visible spectroscopic analysis of the carrageenan aqueous solution and AuNPs synthesized was performed at room temperature in a Jasco Spectometer *V*-670 (JASCO, Tokyo, Japan) employing a wavelength range between 200 and 800 nm.

A ZetasizerNano S (Malvern Instruments, Malvern U.K.) was employed for the determination of the zeta potential of AuNPs to analyze the stability and the charge of the colloidal suspension.

For the characterization of the size and shape of the nanoparticles synthesized transmission electron microscopy (TEM) images were acquired. First, for the preparation of the samples, it was necessary to eliminate part of the organic fraction of the samples. The AuNPs sampled were centrifuged at 10000 rpm for 30 min, the supernatant was discharged and the nanoparticles pellet was redispersed in milli-Q water. Then a drop of this solution was deposited on a 400 mesh copper grid coated with formvar and carbon and onto a holey carbon film supported on a copper grid.

Low magnifications TEM images were acquired in a JEOL JEM 1010 microscope (JEOL, Tokyo, Japan) working at 100 kV. While high resolution TEM (HRTEM) and scanning transmission electron microscopy images were acquired using a JEOL JEM 2010F field-emission gun TEM (JEOL, Tokyo, Japan) operating at 200 kV. Oxford Inca Energy 200 (Oxford Instruments Analytical, UK) was employed for the acquisition of elemental maps in STEM mode. Digital Micrograph software by Gatan was used for data acquisition and analysis, and ImageJ package for the determination of the particle size and mean size distribution calculated from the low resolution TEM images.

2.10.9. Statistical study

Variance analysis (ANOVA) was employed to the statistical analyze of the obtained data using PASW Statistics software (*v*.22, IBM SPSS Statistics, USA). Whenever differences between averages were identified during the variance analysis, a Scheffé analysis was performed to differentiate means with a 95% confidence ($p < 0.05$),

3. Results and discussion

3.1. Hydrothermal treatment of Chondrus crispus with subcritical water

The influence of the final heating temperature during nonisothermal operation on the global extraction yield showed a continuous increase from 73.98% at 120 °C to 89.73% at 200 °C (Fig. 2.a), a value in the range of those attained from *Hypnea musciformis* (up to 81%) operating at 210 °C for 10 min [35]. However, the recovered crude carrageenan after ethanol precipitation showed a maximum of 75.50% at 140 °C and a marked decrease to 55.84% at 160 °C. In our study no carrageenan could be recovered after ethanol precipitation of the liquid phase produced at higher temperatures. Comparable carrageenan yields have been reported from *Kappaphycus alvarezii* operating at 120–180 °C in a treatment consisting on heating and maintaining the target temperature for (5–60 min), and higher values could be attained at higher temperatures and time [36] when an ionic liquid was added [5]. The maximum extraction yield under atmospheric conditions was under 40% when extraction was performed with distilled water at 85 °C for 4 h [9], in the presence of alkali (70%) [37] or assisted by ultrasound (44.30%) [26].

The carrageenan-free extracts showed that glucose was the major saccharide at 120 °C and galactose was maximal at 160 °C (Fig. 2.b). The carrageenan impurities of the fraction precipitated, according to interpretation of NMR data, were 6.8% at 120 °C, 4.6% at 140 °C and 3.1% at 160 °C. At higher temperatures the composition in Fig. 2.b refers to the whole extract and the abrupt decrease from 180 °C to 200 °C suggested that thermal degradation of the saccharidic fraction and cleavage of sulfate groups occurred. The average molecular weight of the major peak in the carrageenan free extracts was progressively reduced with temperature, except at 120 °C (Fig. S1), where the wide dispersion of average molecular weight values has been ascribed to the presence of nonhydrolyzed molecules, probably due to weak intensity hydrolytic processes [11]. The signal intensity was markedly lowered at 200 °C and the extracts at 120–160 °C showed two peaks, the first at higher

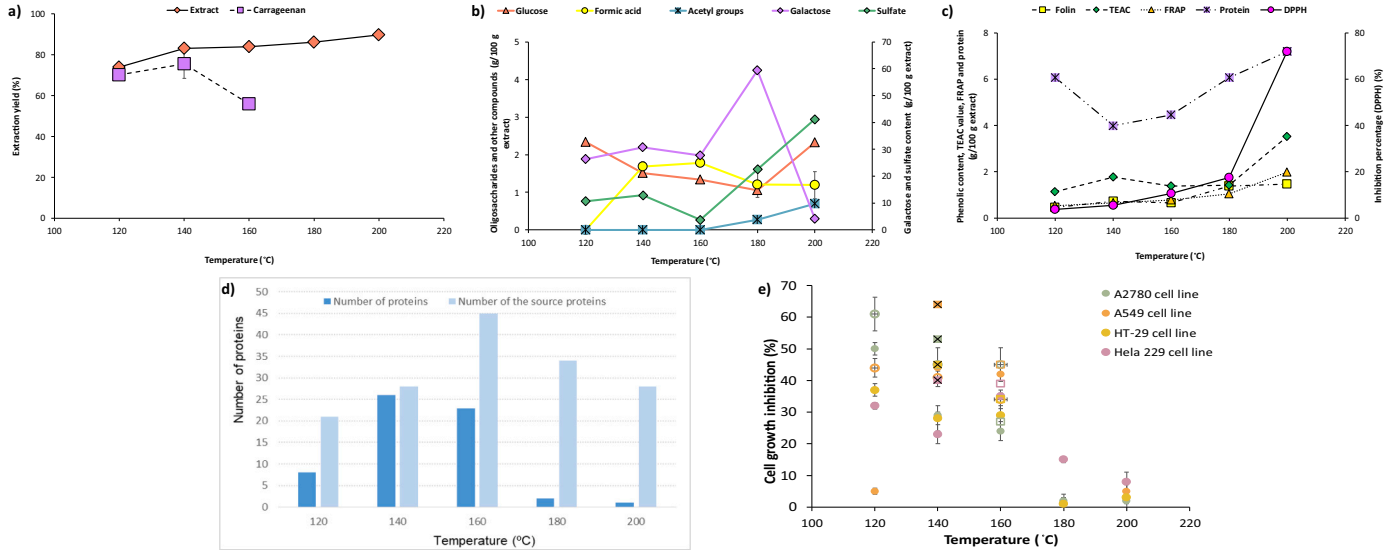

Fig. 2. Influence of the hydrothermal treatment temperature on a) the yield of extract and crude carrageenan; b) saccharidic and sulfate content (note that for 120–140 °C is the carrageenan free extract) and c) phenolic and protein content and antioxidant properties in the freeze-dried *C. crispus* extracts; d) number of proteins and number of source proteins of the free peptides in the ammonium acetate/methanol precipitate from extracts, and e) Cytotoxic action of the *C. crispus* hydrothermal extracts (full) and the precipitated carrageenan fraction (empty symbols), sonicated samples (X) and >100 kDa (square) evaluated at 0.1 mg/mL on selected cancer cell lines, ovarian (A2780), lung (A549), colon (HT-29) and cervical (Hela 229).

molecular weight.

The phenolic content of the carrageenan-free extract showed an increase from 0.5 to 2 g GAE/100 g extract with the extraction temperature in the studied range (Fig. 2.c). The antiradical capacity increased at 200 °C, suggesting a change in the active structures, composition of the extracts or the formation of reaction products. Similar behavior with maximal antioxidant capacity at 210 °C was reported for *H. musciformis*. An expected analogous behavior was observed for the reducing power. The antioxidant activity could be due to phenolics and also to peptides, which are highly active. The protein content in the carrageenan-free extract showed a slight increase at higher temperature, reaching 7% of the extract at 200 °C, suggesting that 70% of the initial protein was solubilized (Table S1). Such behavior is expected during subcritical water extraction, due to the intracellular location of proteins and the cohesion with polysaccharides [5,35,38,39]. SDS-PAGE analysis of precipitated proteins showed, in all tested samples, weak or missing protein bands (Fig. S2) suggesting that a protein hydrolyzation occurred following the heating treatments. Low molecular weight signals were identified close to the bottom of the gel showing the presence of low mass proteins in the hydrolysates. LC-MS/MS analyses showed a distinct distribution in the number of proteins identified in *C. crispus* samples (Fig. 2.d) revealing that the amounts of hydrolyzed proteins and peptides extracted strongly depends on the temperature used. 26 and 23 were the highest numbers of proteins identified in precipitated samples from extracts processed at 140 and 160 °C, respectively, whereas operating at 160 °C allowed the extraction and detection of the greatest number of free peptides (58 peptides generated from 45 proteins) (Fig. 2.d). Among all proteins identified in each condition, most of the proteins were phycobiliproteins like phycocyanins and phycoerythrins, and ribulose bisphosphate carboxylases (unpublished data). Currently, phycobiliproteins are largely utilized in various commercial sectors as supplementary additives in foods beverages and cosmetics [40,41]. They also have several health-promoting properties including antioxidants, antibacterial, anticancer, antiinflammatory, hepatoprotective, hypocholesterolemic, neuroprotective and immune modulator activities [42–44]. The green extraction technology used in this work, especially with temperatures between 140 and 160 °C, has proven to be effective to extract hydrolyzed proteins of high biological value like phycobiliproteins.

The waste solids remaining after the hydrothermal treatment was mainly composed of the mineral fraction, which accounted for 26% of the solid remaining after extraction up to 120 °C, and was progressively lowered after hydrothermal treatments at higher temperature (Table S1).

3.2. Cytotoxic activity on tumoral cells

Food grade carrageenans, showing molecular weights in the range 200–800 kDa usually exhibit lower cytotoxic activity on tumoral cells than lower molecular weight, degraded carrageenans (10–20 kDa) and chemically modified derivatives [11,45]. Therefore, in an exploratory assay the cytotoxicity of the extracts, evaluated at 0.1 mg/mL showed differences among the cell lines. HT-29 and Hela 229 were the less susceptible, and in the most affected cell lines, the crude carrageenan separable by ethanol precipitation was probably responsible for this action (Fig. 2.c). The most active was the ethanol precipitated crude carrageenan obtained at 120 °C against A2780 cells ($IC_{50} = 0.0154 \pm 0.002$ mg/mL). The conventionally extracted carrageenan showed 48% inhibition on A2780 and 32% on A549 cells. The highly degraded fractions obtained at 180 and 200 °C were ineffective. The selected cell lines also showed different susceptibility to cisplatin (69–96%) with IC_{50} values of 0.62 μM (A2780), 9.8 μM (A549), 18.9 μM (HT29) and 0.80 μM (Hela 229). The low activity could be explained by the high molecular weight (100 kDa) (Fig. S1), comparable to those of commercial products. In order to avoid excessive degradation at temperatures higher than 140 °C, a sequence of subcritical water extraction and further posthydrolysis was also tried following a previously developed approach assisted by ultrasound [46] or by microwave [47]. After ultrasound assisted treatment of the subcritical water extracts from 140 °C, a slight increase in the cell growth inhibition was observed, reaching 53% in ovarian cancer cells (A2780), 64% in lung (A549), 45% in colon adenocarcinoma (HT-29) and 40% in cervical cancer cells (Hela 229). However, the antiproliferative action was lower than for samples directly extracted by ultrasound assisted processes, with > 90% cell growth inhibition and EC_{50} under 0.05 mg/L [26].

3.3. Membrane fractionation of the extracts

At operation temperatures higher than 160 °C carrageenan could not be recovered from the extracts by ethanol precipitation. Therefore, fractionation in ultrafiltration membranes was proposed to determine the influence of the final operation temperature on the molecular weight distribution and properties of extracts produced under two different conditions. Whereas the fraction retained in the 100 kDa membrane accounted for 57% of the extracts produced at 160 °C, this fraction was only 1% of the extract obtained at 200 °C (Fig. 3.a). The recovery yield from the 160 °C extract accounted for 48.5% of the dry seaweed, lower than the crude carrageenan yield precipitated with ethanol was 55.8% (Fig. 2.a).

The HPSEC profile of the 100 kDa retentate of the extract produced at 160 °C showed a dispersion in the molecular weight (Fig. S2), the profile exhibits a peak higher than 277 kDa, and another one lower than 23 kDa, which was probably retained in the cake layer formed during ultrafiltration. The profiles of the fractions from the extract obtained at 200 °C showed lower intensity and except for the 100 kDa, with values under 24 kDa (Fig. S3.a and S3.b).

The FTIR signals at 845 and at 930 cm^{-1}, more intense for the higher molecular weight fractions, were not present in the samples from 200 °C, confirming the galactose and 3,6-anhydrogalactose degradation under these conditions (Fig. S4). The complete cleavage of sulfate groups can also be inferred from the lack of signals in the 200 °C samples at 1230–1260 cm^{-1}, associated with the total number of sulfate groups [11,48].

The phenolic content in the retentates from hydrothermal extracts obtained at 160 °C was maximal in the 1 and 3 kDa membranes, accounting for only 0.7% of the retentate product, whereas from the extract produced at 200 °C represented up to 2.5% of the retentate. The TEAC values of fractions under 100 kDa were slightly improved compared to those of the unfractionated extracts, but overall values remained low (Fig. 3.b). As a general trend, the fractionation of carrageenan and protein was not feasible. In the 50–100 kDa fractions obtained from the 160 °C extract, protein accounted for 2.3% of the dry weight, whereas the major fraction of the 200 °C extract corresponded to the 30–50 kDa.

Only the retentate in the 100 kDa membrane of the extract produced at 160 °C was evaluated for antiproliferative properties. The cell growth inhibition caused by the >100 kDa fraction was low, ovarian (27%), lung (45%), colon (34%) and cervix (39%). Despite the lower molecular weight of the extract obtained at 200 °C, the antiproliferative action was low (Fig. 2.e). However, the fractions obtained at 220 °C showed antiviral properties against aquaculture virus and also plant growth biostimulant action (unpublished data). Therefore, in order to maintain high extraction yield compared to conventional processes, with low carrageenan degradation and also achieving the extraction of other bioactives, such as phenolics and peptides with antioxidant properties, operation should be carried out at 140 °C. In case further depolymerization is desired, an additional stage, preferably assisted by microwave or ultrasounds should be proposed. Since the aim of this study was to achieve an efficient use of the raw material, operation at 140 °C was selected to produce a crude extract that was tried for the formulation of gold nanoparticles, based on their content in carrageenan as stabilizing agent and phenolics and protein as reducing agents. The formulation of

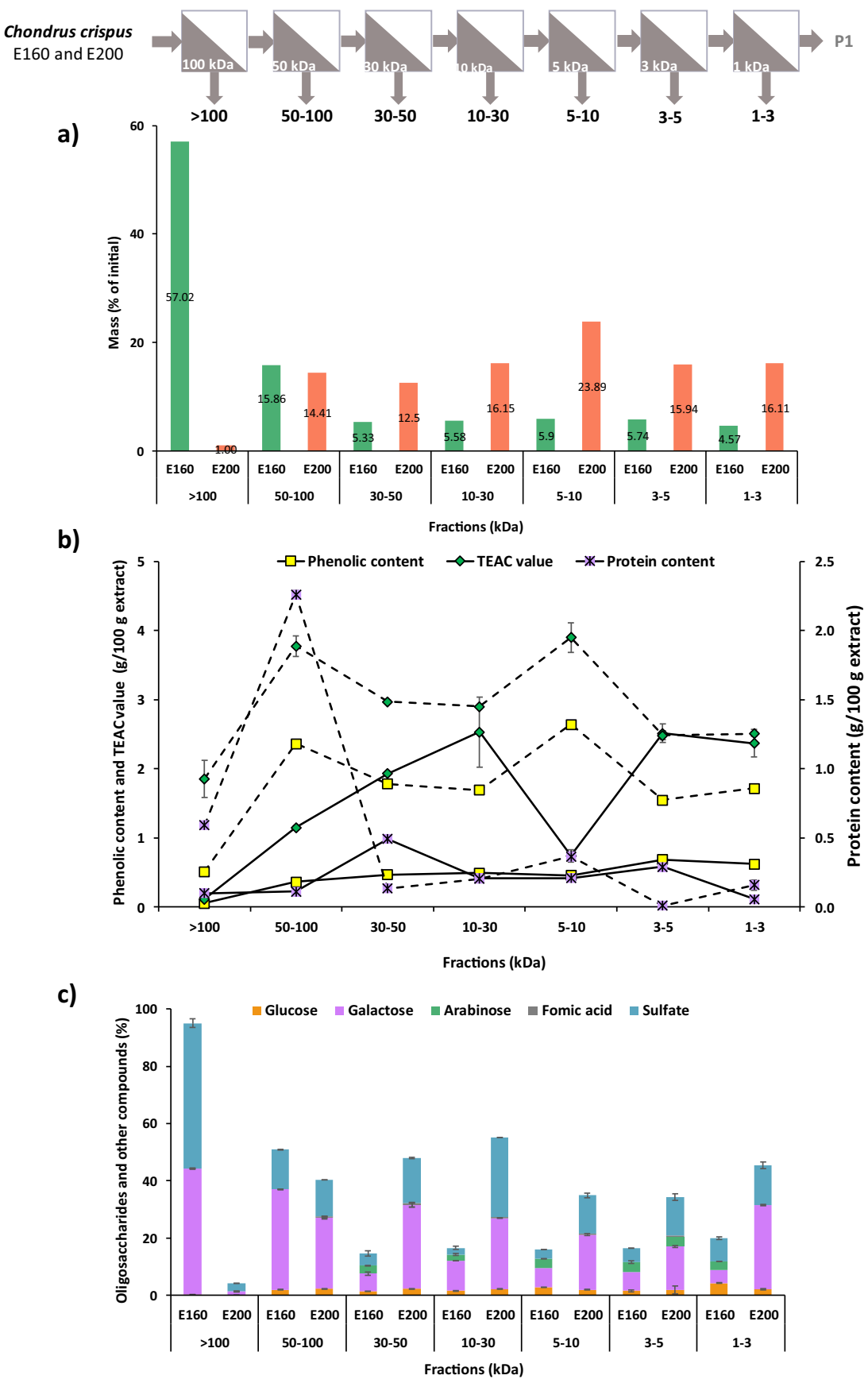

Fig. 3. Membrane fractionation of the extracts, a) mass fraction recovered in each membrane, b) phenolic and protein content and antiradical properties and c) distribution of the saccharidic compounds, sulfate and degradation products of the retentates from the extracts obtained at 160 °C (continuous) and at 200 °C (dotted).

hydrogels for 3D printing was also evaluated.

3.4. Rheological features of proposed gelled matrices

The crude carrageenans precipitated from the extracts obtained at 120–160 °C were further characterized. Fig. 4 shows the impact of hydrothermal extraction temperature on the viscoelastic properties of the extracted carrageenans from *C. crispus* to the development of a wide set of gelled matrices, including those processed under 3D printing. It should be indicated that all extracted biopolymers exhibited typical kappa/iota-hybrid carrageenans features (Fig. S5), with the characteristic FTIR absorption bands at 803 cm^{-1} (3,6-anhydro-galactose-2-sulfate, iota), 845 cm^{-1} (δ-galactose-4-sulfate, both kappa and iota), 925 cm^{-1} (3,6-anhydro-galactose, kappa) and at 1240–1220 cm^{-1} (ester sulfate group) [11,49]. The molar ratio of main monosaccharides (A_{1070}), 3,6-AnGal (A_{930}), and sulfate (A_{1258}) calculated from the IR spectra are summarized in Table S2.

The obtained values show a lower 3,6-anhydrogalactose content, compared to those of [11], who reported a molar ratio Gal: 3,6-AnGal: SO_4^{2-} of 1:0.9:0.73 for κ-Carrageenan from *C. armatus*, and slightly lower for the low molecular weight oligomers obtained by mild acid hydrolysis, in 0.1 M HCl or by autohydrolysis of λ-carrageenan in distilled water and incubated for 24 h at 37 °C, with 1:0.83:0.78. However, hydrophobicity is due to 3,6-anhydrogalactose and this property in the solvent increased with operation temperature [16]. Gereniu et al. (2018) proposed subcritical water extraction and also combined with ionic liquids, but both provided lower gel strength than conventional extraction [5]. Probably conventional caused a partial elimination of sulfates from the beta-1,4-linked galactose due to the increased pH under alkaline conditions that created the 3,6-anhydrogalactose gel form units. Torres et al. (2021) reported ratios of 1:0.59:0.95 for k/i-hybrid carrageenans extracted from *C. crispus* after ultrasound treatment with potential antiproliferative properties [26].

The hybridization degree (iota/kappa) of recovered carrageenans, calculated from the ^{1}H NMR peaks corresponding to the fractions of iota- and kappa-disaccharide units, was 0.28 ± 0.1 consistently with values found for hybrid carrageenans extracted under conventional alkali treatments from the same seaweed (kappa: 78 and iota: 22) [50]. Also, HPSEC profiles of hybrid carrageenans extracted after hydrothermal treatment at 120 °C presented a double peak at 2.8 10^5 g/mol shifted at higher average molecular weights with increasing hydrothermal temperature up to 160 °C. These values are in the range of those previously reported for hybrid carrageenans recovered from similar carrageenophyte seaweeds (8 10^3 and 2.2 10^6 g/mol) highly depending on the extraction conditions [24].

Fig. 4.a presents the viscoelastic behavior of gelled matrices prepared with the extracted hybrid carrageenans depending on the used counterion (K^+, Ca^{2+}). All systems exhibited typical gel profiles with the viscous modulus, G″, lower than elastic modulus, G′, and almost frequency independent, except for those prepared in the presence of Ca^{2+} with the carrageenans extracted from hydrothermal liquids treated at 160 °C. The strength of the gelled matrices increased for carrageenans obtained after milder hydrothermal processing conditions. Even though, those formulated with K^+ counterions exhibited higher viscoelastic properties (3-fold) than those prepared with Ca^{2+}. This behavior suggests that K^+ counterions with higher van der Waals radium promote the

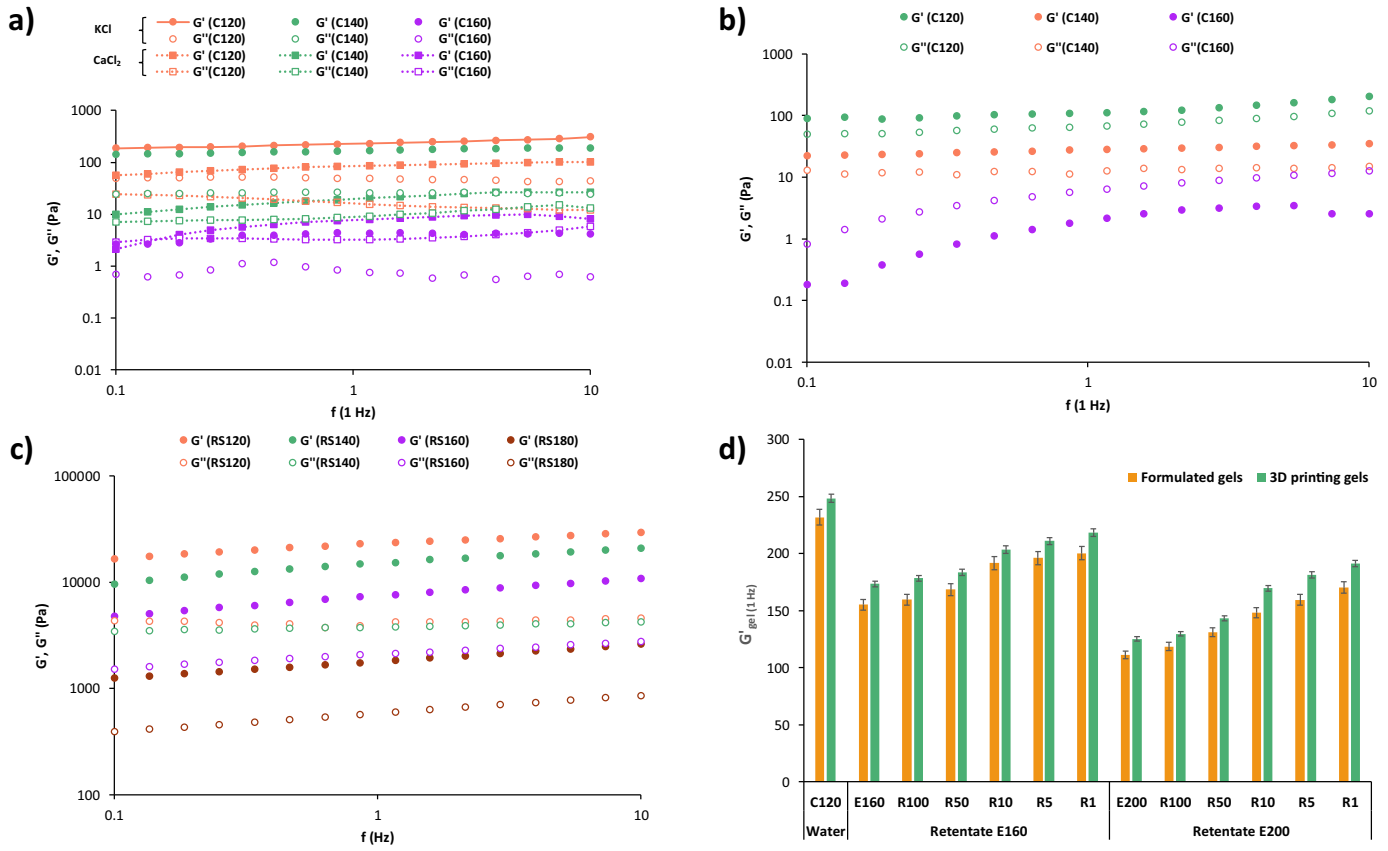

Fig. 4. Influence of the extraction temperature on the rheological properties of the proposed hybrid carrageenan gelled matrices. Plot (a) shows the impact of the type of salt (KCl, $CaCl_2$) at fixed biopolymer (1%) and ionic strength (0.1 M) using water as solvent on the developed gels. Plot (b) presents the effect of using the liquid extract of 200 °C as solvent for the formulation of above gels (KCl 0.1 M, 1%). Plot (c) displays the influence of recovered solids (RS) (10%) in the development of selected carrageen gels (KCl_120, 0.1 M, 1%) using water as solvent. Plot (d) shows the impact of 3D printing on the viscoelastic behavior in terms of $G'_{0\ (1Hz)}$ of representative gelled matrices (*i.e.* gelling agent: KCl_120, 0.1 M, 1%; and solvent: retentates from hydrothermal extracts (160 and 200 °C) from >100 to 1–3).

effect in gel structure strengthening due to the highest impact on the gel stabilization process [51].

Fig. 4.b shows the impact of using as solvent the liquid extract of 200 °C on the mechanical spectra of gelled matrices made with representative hybrid carrageenans (KCl 0.1 M, 1%). Note here that permeates and retentates from hydrothermal extracts (160 and 200 °C) after fractionation in ultrafiltration membranes and MHG liquid extracts were also tried with similar results. Typical gel behavior was maintained in the systems prepared with hybrid carrageenans from hydrothermal treatment at 120 and 140 °C, whereas liquid-like profiles were identified for those made with biopolymers extracted from hydrothermal processing at 160 °C. The magnitude of both viscous and elastic moduli dropped (2-fold) when compared with those formulated using water as solvent. This tendency suggests a competition by free water between the biopolymers used as gelling agents and the highly hygroscopic solid extracts present in the hydrothermal liquids used as solvents as previously found for other gelled matrices incorporated with different ingredients [52].

Fig. 4.c presents the effect of recovered solids after hydrothermal treatment of *Chondrus crispus* on the rheological properties of selected gelled matrices made with the hybrid carrageenans that exhibited the highest gel strength (KCl_120, 0.1 M, 1%). In all cases, the incorporation of residual solids involved a rise in the viscoelastic properties (about 100-fold) of the selected gels without jeopardizing the characteristic gel behavior of the proposed systems. At fixed frequency, both G′ and G″ moduli decreased with increasing hydrothermal temperature of the used solids, mainly for those coming from the most sever treatments. No gelled matrices were obtained at proposed conditions with solids from seaweed processing at 200 °C. It should be indicated that absence of syneresis was observed in all gelled matrices after 2 weeks of cold storage, which is a relevant issue from the industrial point of view [27].

Design of novel 3D printable gels was proposed based on the incorporation of different fractions (*i.e.* AH liquid extracts as well as the corresponding retentates and permeates, MHG liquids, recovered solids or nanoparticles) in the formulation of gels. As representative example of all tested systems, Fig. 4.d displays the potential of proposed carrageenan systems to be used in an emerging technology as 3D printing. The comparison between the viscoelastic properties, in terms of $G'_{gel\ (1\ Hz)}$ for both the formulated hybrid carrageenan gelled matrices and the corresponding prepared by 3D printing were displayed. In all cases, an enhancement (about 10-fold) of the gel strength was observed for hybrid carrageenan gelled matrices formulated using this emerging technology, independently of the liquid phase used as solvent. This behavior suggests that relatively high temperature together with low speed and layer height promote the structuring of hybrid carrageenan involving increase to gel networks with stronger interactions. The rheological response of printable gelled matrices previously reported with k-carrageenan using a RepRap 3D printer, indicated a slight frequency dependence of G′ modulus and a soft minimum in the evolution of the G″ modulus [22]. Again, no water syneresis was identified for printable gels after 2 weeks of cold storage.

The interest of incorporation of phenolic compounds to biobased polymers is well known, commonly between 1 and 4%, which is consistent with the values proposed here (up to 2%). The interest in supplementation of phenolics on films and coatings for food packaging is based on the oxidative stabilization of package and products and to other additional activities. The added polyphenol extracts influence on physical appearance and structure, mechanical and barrier properties, sensorial and biological functions, such as antioxidant and antimicrobial. However, the addition of polyphenols and extracts caused darkening of polysaccharide based films, and excessive addition in κ-carrageenan films could decrease the tensile strength and thermal stability [53].

Those hybrid carrageenan-based gels printed in this study using as solvent hydrothermal liquid extracts, the corresponding permeates or retentates, and MHG liquid extracts presented compatible mechanical properties with those reported for films and coatings for food packaging [8,13,54]. Printable matrices incorporated with nanoparticles could be interesting composites for wound dressing [55], whereas those prepared using recovered solids for exfoliate or face masks [56]. In general, this biopolymer is recognized as safe (GRAS) and is a food additive (E-407), based on a history of use and toxicology studies. Food-grade carrageenan (average Mw > 100 kDa and not >5% below 50 kDa) is not degraded nor absorbed in the gastrointestinal tract. Low molecular weight carrageenan exhibits toxicological properties at high doses and can induce gastrointestinal irritation [57].

3.5. Synthesis and characterization of gold nanoparticles

The extract obtained during heating up to 140 °C, optimal regarding extraction yield, gelling and reducing properties was selected for the optimization of the synthesis of AuNPs. First, several attempts were performed at room temperature (RT) with different concentrations of carrageenan and a fixed concentration of Au(III) (0.4 mM). Unfortunately, no color change was observed after 72 h and the acquisition of the UVVis spectra did not show the formation of nanoparticles (Fig. S6. a).

Previous studies suggested that carrageenan needs basic medium to be able to reduce Au(III) to Au(0) [58–60], even though in our previous study employing carrageenan extracted from the red seaweed *Mastocarpus stellatus* to synthesis AuNPs it was not necessary to add NaOH [61]. Then, since our extract is rich in carrageenan, the same reaction conditions were performed but NaOH (0.01 M) was added to the extract solution until pH 11 and then HAuCl4 was added. After 24 h of reaction a color change was observed in the reaction employing the lowest concentration of extract. However, it can be observed in the UV–Vis spectra that the surface resonance band of gold is too wide (Fig. S6.b).

In order to evaluate the effect of the temperature in the synthesis, reactions with the same concentration of carrageenan (0.25 mg/mL) and of gold (0.4 mM) were performed at room temperature, 60 and 90 °C with and without NaOH. It can be observed in Fig. 5.a that the reaction only took place at 90 °C with and without NaOH and when heating at 60 °C with NaOH. However, it should be noted that the surface resonance band of gold is narrower in the synthesis performed at higher temperature. Also, the position of the maximum wavelength shifted affected by the temperature of reaction and by the addition or not of NaOH, appearing at 559 nm at 60 °C and at 525 nm and 543 nm at 90 °C with and without NaOH respectively.

To observe the effect of the addition of NaOH in the synthesis of nanoparticles, transmission electron microscope images were acquired for the samples obtained heating at 90 °C (Fig. S7). It can be observed that the nanoparticles synthesized without NaOH are bigger and pseudospherical with mean diameter of 44.7 ± 10.1 nm while when using basic medium, the nanoparticles obtained are smaller, spherical and with narrower size distribution with a mean size of 8.4 ± 0.9 nm.

Once the optimal temperature and pH has been stablished, it is necessary to optimize the concentration of extract. Three new syntheses were performed with concentrations of extract of 0.25, 0.125 and 0.04 mg/mL, with a fixed concentration of gold of 0.2 mM, at pH 11 and 90 °C. From Fig. 5.b, it can be observed that the concentration of the extract greatly affects the synthesis of the nanoparticles. As the concentration decreases, the band shifts to longer wavelengths and becomes wider. The maximum of absorbance wavelength shifts from 525 nm with a concentration of 0.25 mg/mL to 568 and 600 nm with concentrations of 0.125 and 0.04 mg/mL, respectively. The differences observed in the position and appearance of the SPR band is also reflected in the size and shapes of the nanoparticles obtained as shown in the TEM images (Fig. S8). When decreasing the concentration of extract, the nanoparticles formed are irregular in sizes and shapes and significantly bigger.

Regarding the optimal gold concentrations, different reactions were performed with concentration of gold(III) ranging from 0.16 to 0.40

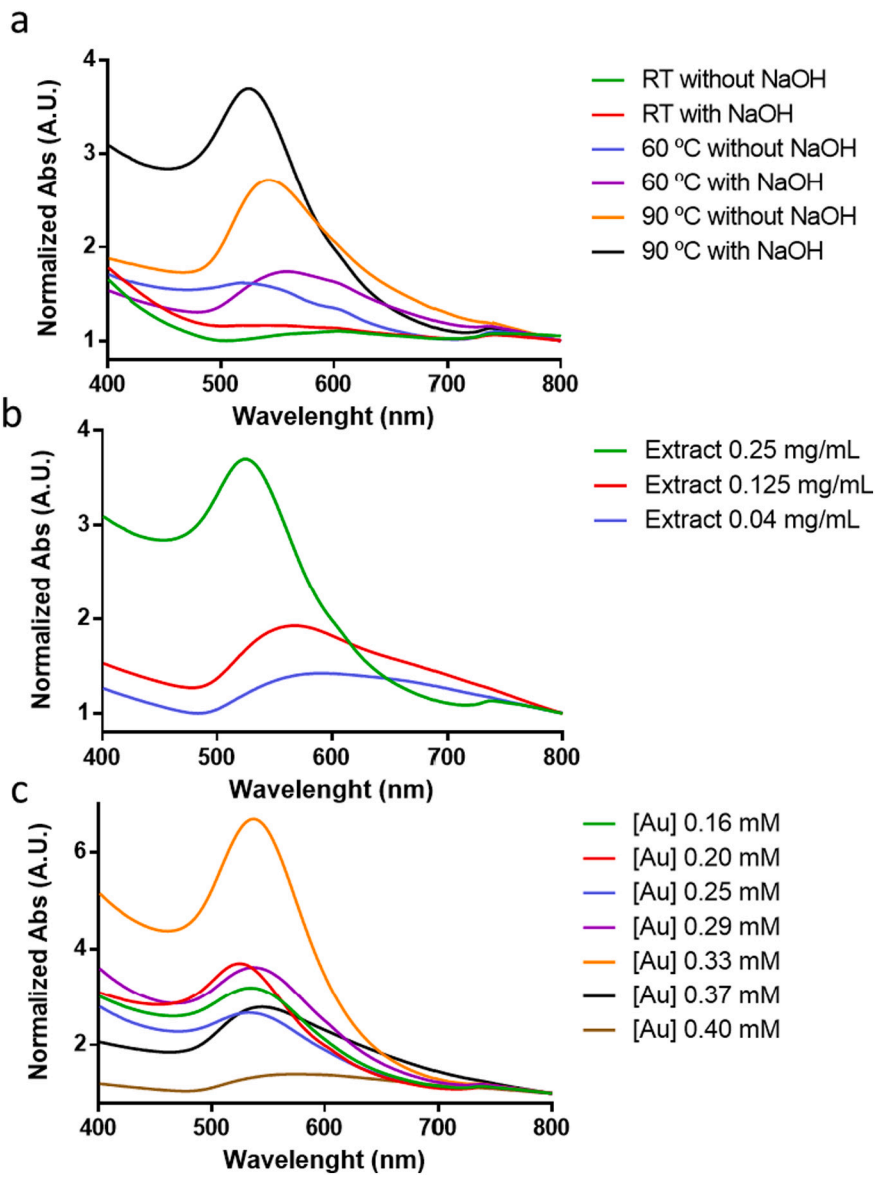

Fig. 5. UV–Vis spectra of a) reactions with the same concentration of extract (0.25 mg/mL) and of gold (0.4 mM) at RT, 60 and 90 °C with and without NaOH b) concentrations of extract of 0.25, 0.125 and 0.04 mg/mL, with a fixed concentration of gold of 0.2 mM, at pH 11 and 90 °C and c) concentration of gold(III) ranging from 0.16 to 0.40 mM, at the fixed concentration of extract of 0.25 mg/mL at 90 °C and pH 11.

mM, at the fixed concentration of extract of 0.25 mg/mL at 90 °C and pH 11 (Fig. 5.c). It can be observed that the reactions occurred at all the gold concentration tested, however, it should be noted that with the two higher concentrations of gold the SPR band obtained is less intense and broader, this could be explained since it was observed that part of the nanoparticles precipitated, indicating that this concentration of carrageenan is not able to stabilize such high concentrations of gold. From the UV–Vis spectra it was not possible to stablish any conclusions regarding the effect of the concentration of gold in the synthesis of nanoparticles since a regular pattern is not observed. However, in TEM images (Fig. 6) it can be observed that with lower concentrations of gold the nanoparticles are spherical and smaller while when the concentration of gold is increase it can be observed the appearance of bigger, pseudo-spherical particles and mixtures of small and bigger nanoparticles.

In view of the results obtained, the optimal synthesis conditions have been selected to be 0.25 mg/mL of extract, 0.2 mM of $HAuCl_4$, pH 11 and 90 °C to obtained spherical nanoparticles with mean size of 8.4 ± 0.9 nm. The nanoparticles obtained at these conditions have been fully characterized with different techniques.

First, to study the stability and the charge of the colloidal suspension Z potential measurements have been acquired, obtaining a mean value of −40.2 ± 1.9 mV (Fig. S9). These results indicate that the nanoparticles synthesized are highly stable, forming a colloidal suspension that carries a negative charge possibly due to the carrageenan. It is noteworthy to highlight the formation of such stable nanoparticles with such small size, since nanoparticles smaller than 10 nm are difficult to produce and stabilize.

This high stability might be due to the carrageenan present in the extract acting as an organic matrix that prevent the gold nanoparticles to aggregate. This can be observed in the STEM image acquire (Fig. 7.b) where it can be observed that the gold nanoparticles (bright contrast) are surrounded by a matrix with less contrast. The EDX (Fig. 7.a) and the mapping performed (Fig. 7.c,d,e,f) confirmed the organic nature of this matrix. The EDX Analysis performed further confirmed that carbon, calcium, chlorine, oxygen, and potassium were present in the sample as well as gold. Although this seaweed can also possess metals and other compounds, the peaks observed in the spectra of copper are due to the metal grid employed and the silicon peaks are from the microscope

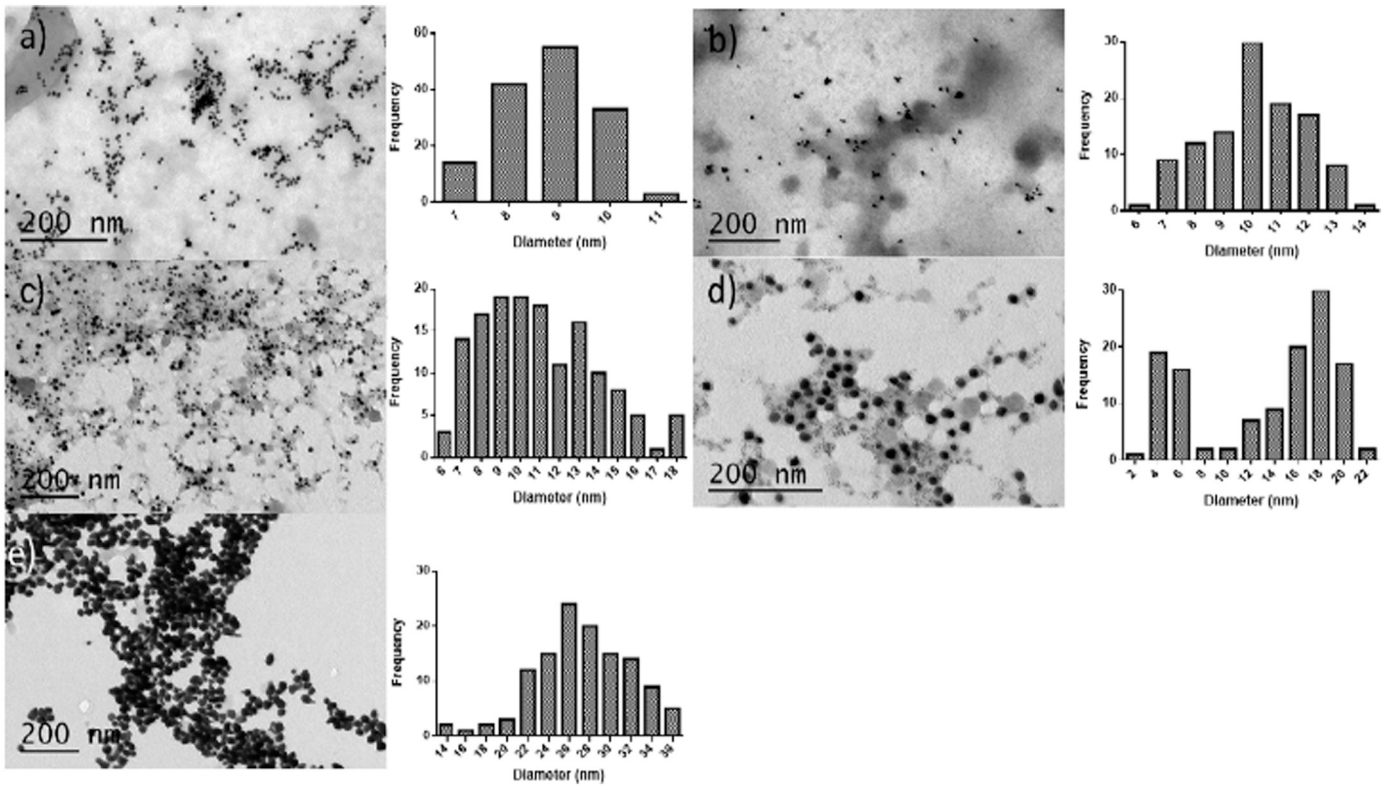

Fig. 6. TEM images of AuNPs synthesized at the fixed concentration of extract of 0.25 mg/mL at 90 °C and pH 11 and concentration of gold a) 0.2 mM b) 0.25 mM, c) 0.29 mM, d) 0.33 mM and e) 0.39 mM, with their corresponding size distribution histogram.

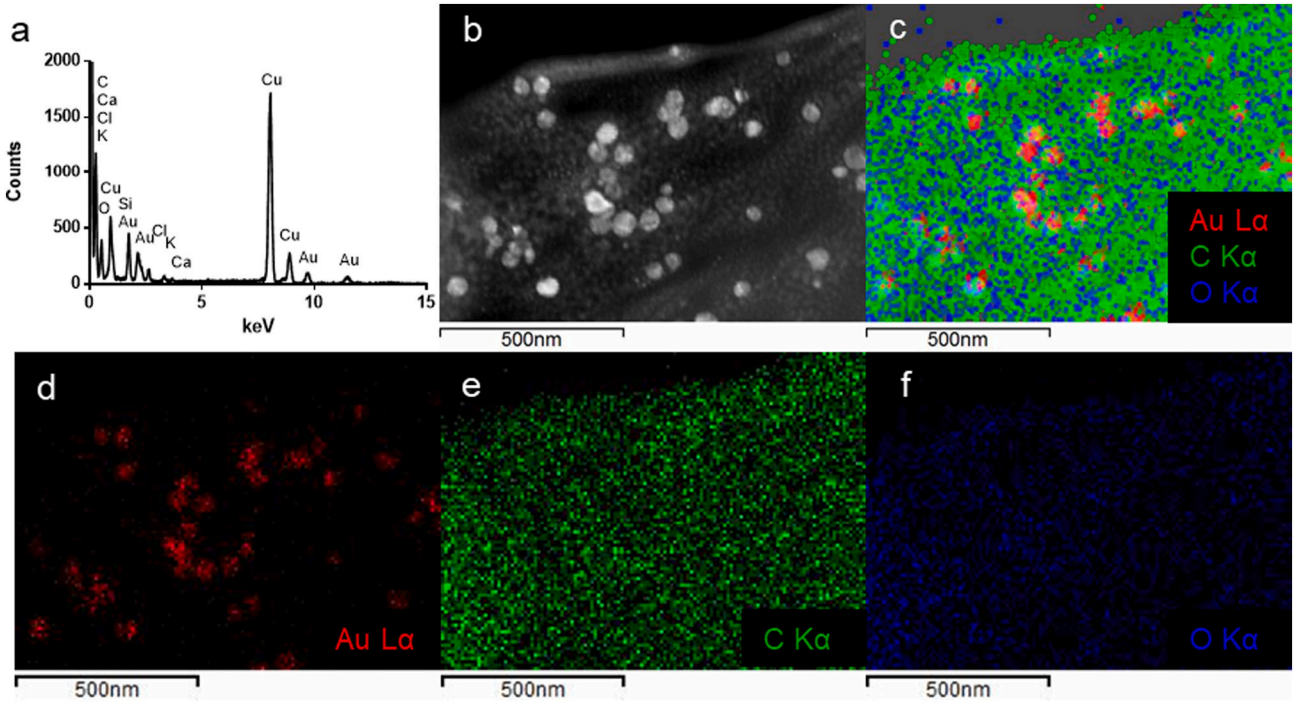

Fig. 7. a) EDX spectrum b) STEM images, c, d e and f) elemental mapping of AuNPs.

detector.

The crystallinity of the synthesized nanoparticles was analysed by means of HRTEM. The selected area electron diffraction (SAED) analysis (Fig. 8.a) revealed the crystalline nature of the nanoparticles in the form of circular rings form by irregular dots with lattice spacing corresponding to (111), (002), (022), (113) and (133) planes of the face centered cubic lattice structure of gold. This ring pattern is associated with polycrystalline materials.

In Fig. 8.b is shown an example of a nanoparticle that crystalize in a decahedral quasi-spherical shape, along with the FT of the nanoparticle

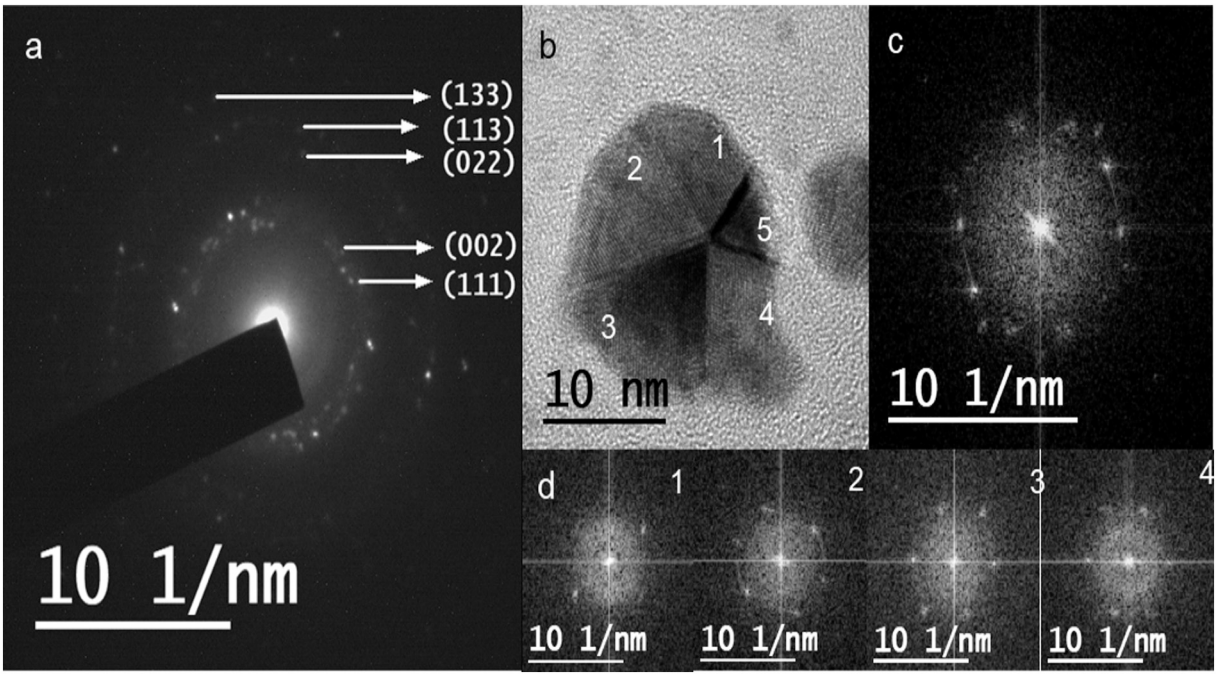

Fig. 8. a) SAED of AuNPs b) HRTEM image of a decahedral quasi-spherical nanoparticle c) Fourier Transform of b) d) Fourier transform of each region marked in b).

(Fig. 8.c). In the particle it can be appreciate the five different crystalline domains that form it and in Fig. 8.d are collected the FT of four of these domains. Due to the orientation of the particle, it was not possible to obtaine that of the 5th domain. In all of these domains the preferential d-spacing calculated was 0.23 nm which corresponds to Miller index (111).

Infrared spectroscopical analysis of the extract before and after the synthesis of AuNPs was performed between 4000 and 400 cm^{-1} (Fig. S10). The analysis of the difference in position and intensity of the bands could give information about which functional groups are involved in the reduction of gold and in the capping of AuNPs.

First, regarding the assignation of the bands, in the spectra of the extract before the synthesis, at 3400 cm^{-1} appears the most intense band, assigned to O—H stretching vibrations. At 2900 cm^{-1} appears a weaker band attributed to C—H vibrations. For the assignation of the bands that appears in the region between 1600 and 1400 cm^{-1} in the literature can be found some discrepancies. Some authors assigned the two bands that appears at 1640 cm^{-1} and 1400 cm^{-1} to asymmetrical and symmetrical stretching of carboxylate groups respectively. However, other authors propose that the bands that appears around 1600 and 1550 cm^{-1} appears due to the presence of the functional groups of amide I and II from proteins. Typically, these bands appear overlapped due to the appearance of a strong band at around 1640 cm^{-1} assigned to carbonyl group in the spectra of polysaccharides containing uronic acid. The appearance of a band at 1260 cm^{-1} indicates the presence of sulfate groups in the polysaccharide structure since this band is assigned to asymmetric stretching vibration of sulfated esters. While the glycosidic bond C—O and the sugar ring stretching vibrations are assigned to the signals at ~1000–1100 cm^{-1}. Finally, the region known as fingerprint or anomeric region in the wavenumber interval between 950 and 700 cm^{-1} appears 3 characteristic bands from polysaccharides that are attributed to 3,6-anhydro-galactose residue, galactose-4-sulfate and 3,6-anhydro-galactose-2-sulfate.

The comparison of the spectra of the extract after the synthesis of AuNPs show slight changes in the position, wide and intensity of the band at 3400 cm^{-1} which suggests the participation of hydroxyl groups in the synthesis. Also, it can be noted differences in the bands between 1600 and 1400 cm^{-1} indicating that carbonyl groups can be involved in the synthesis and stabilization of the nanoparticles. Lastly, it is also observed a shift in the band at 1250 cm^{-1} suggesting that the carrageenan present in the extract can bind gold through the sulfur atoms and act as capping and stabilizing agent. The results obtained in this study are in accordance with previous ones that confirmed the participation of hydroxyl groups as the prime reductants of Au(III) into Au(0) [58,60].

4. Conclusions

Hydrothermal processing with subcritical water during non-isothermal heating up to 140 °C provided higher carrageenan yields than conventional alkaline treatment at lower temperature and more prolonged times. Operation at higher temperatures caused degradation and neither ethanol precipitation allowed the recovery of carrageenan nor ultrafiltration allowed fractionation of carrageenan oligomers. The antiproliferative potential of the crude extracts or their ultrasound depolymerized products was moderate. Therefore, in this study gold nanoparticles were synthesized employing *Chondrus crispus* freeze-dried extract obtained by hydrothermal treatment at the optimal temperature of 140 °C. The characterization performed allow the confirmation of the synthesis of spherical, polycrystalline nanoparticles with a mean size distribution of 8.4 ± 0.9 nm and Z potential value of −40.2 ± 1.9 m*V*, indicating the synthesis of highly stable nanoparticles despite its small size. Furthermore, it was confirmed that the nanoparticles are inside the organic matrix of the extract, acting as stabilizing agent preventing their aggregation and avoiding their precipitation. Overall, the proposed 3D processing conditions allowed developing a wide range of relatively weak gels incorporated with antioxidant properties with suitable mechanical properties in a few minutes for potential food and non-food applications, which is a big challenge to develop tailor-made hydrogels tailored to specific requirements.

CRediT authorship contribution statement

Milena Álvarez-Viñas: Data curation, Investigation, Writing – review & editing. **Noelia González-Ballesteros:** Data curation, Formal analysis, Investigation, Writing – original draft, Writing – review & editing. **M. Dolores Torres:** Conceptualization, Data curation, Formal

analysis, Funding acquisition, Investigation, Project administration, Resources, Writing – original draft, Writing – review & editing. **Lucía López-Hortas:** Investigation, Writing – review & editing. **Candida Vanini:** Data curation, Investigation, Writing – review & editing. **Guido Domingo:** Formal analysis, Resources, Writing – review & editing. **M. Carmen Rodríguez-Argüelles:** Formal analysis, Resources, Writing – original draft, Writing – review & editing. **Herminia Domínguez:** Conceptualization, Formal analysis, Funding acquisition, Project administration, Resources, Writing – original draft, Writing – review & editing.

Declaration of competing interest

There are no conflicts to declare.

Acknowledgements

Authors thank the financial support to the Ministry of Science, Innovation and Universities of Spain (RTI2018-096376-B-I00), and to the Xunta de Galicia (Centro singular de investigación de Galicia accreditation 2019–2022 and ED431C 2018/54-GRC) and the European Union (European Regional Development Fund - ERDF) - (Ref. ED431G2019/06). M.A.V. thanks for her predoctoral FPI grant (PRE2019-090567) to the Ministry of Science, Innovation and Universities (Spain). M.D.T. acknowledges for her postdoctoral grant (RYC2018-024454-I) to the Ministry of Science, Innovation and Universities (Spain) and for the funding support (ED431F 2020/01) to Xunta de Galicia.

Appendix A. Supplementary data

Supplementary data to this article can be found online at https://doi.org/10.1016/j.ijbiomac.2022.02.145.

References

[1] F.M. Kerton, Y. Liu, K.W. Omari, K. Hawboldt, Green chemistry and the ocean-based biorefinery, Green Chem. 15 (2013) 860–871, https://doi.org/10.1039/c3gc36994c.
[2] C. Filote, S.C.R. Santos, V.I. Popa, C.M.S. Botelho, I. Volf, Biorefinery of Marine Macroalgae Into High-tech Bioproducts: A Review, Springer International Publishing, 2021, https://doi.org/10.1007/s10311-020-01124-4.
[4] M.D. Torres, S. Kraan, H. Domínguez, Seaweed Biorefinery, 2019, https://doi.org/10.1007/s11157-019-09496-y.
[5] C.R.N. Gereniu, P.S. Saravana, B.S. Chun, Recovery of carrageenan from Solomon Islands red seaweed using ionic liquid-assisted subcritical water extraction, Sep. Purif. Technol. 196 (2018) 309–317, https://doi.org/10.1016/j.seppur.2017.06.055.
[6] P. Pérez-Larrán, M.D. Torres, N. Flórez-Fernández, E.M. Balboa, A. Moure, H. Domínguez, Green technologies for cascade extraction of *Sargassum muticum* bioactives, J. Appl. Phycol. 31 (2019) 2481–2495, https://doi.org/10.1007/s10811-018-1725-6.
[7] M. Francavilla, S. Intini, L. Luchetti, R. Luque, Tunable microwave-assisted aqueous conversion of seaweed-derived agarose for the selective production of 5-hydroxymethyl furfural/levulinic acid, Green Chem. 18 (2017) 5971–5977, https://doi.org/10.1039/c6gc02072k.
[8] F.D.S. Larotonta, M.D. Torres, M.P. Gonçalves, A.M. Sereno, L. Hilliou, Hybrid carrageenan-based formulations for edible film preparation: benchmarking with kappa carrageenan, J. Appl. Polym. Sci. 133 (2016), https://doi.org/10.1002/app.42971.
[9] M.G. Tasende, M. Cid, M.I. Fraga, Spatial and temporal variations of *Chondrus crispus* (Gigartinaceae, Rhodophyta) carrageenan content in natural populations from Galicia (NW Spain), J. Appl. Phycol. 24 (2012) 941–951, https://doi.org/10.1007/s10811-011-9715-y.
[10] J.L. Jiang, W.Z. Zhang, W.X. Ni, J.W. Shao, Insight on structure-property relationships of carrageenan from marine red algal: a review, Carbohydr. Polym. 257 (2021), 117642, https://doi.org/10.1016/j.carbpol.2021.117642.
[11] E. Cicinskas, M.A. Begun, V.A. Tiasto, A.S. Belousov, V.V. Vikhareva, V. A. Mikhailova, A.A. Kalitnik, In vitro antitumor and immunotropic activity of carrageenans from red algae Chondrus armatus and their low-molecular weight degradation products, J. Biomed. Mater. Res. A. 108 (2020) 254–266, https://doi.org/10.1002/jbm.a.36812.
[12] H.J. Bixler, H. Porse, A decade of change in the seaweed hydrocolloids industry, J. Appl. Phycol. 23 (2011) 321–335, https://doi.org/10.1007/s10811-010-9529-3.
[13] M. Manzoor, J. Singh, J.D. Bandral, A. Gani, R. Shams, Food hydrocolloids: functional, nutraceutical and novel applications for delivery of bioactive compounds, Int. J. Biol. Macromol. 165 (2020) 554–567, https://doi.org/10.1016/j.ijbiomac.2020.09.182.
[14] R. Yegappan, V. Selvaprithiviraj, S. Amirthalingam, R. Jayakumar, Carrageenan based hydrogels for drug delivery, tissue engineering and wound healing, Carbohydr. Polym. 198 (2018) 385–400, https://doi.org/10.1016/j.carbpol.2018.06.086.
[15] A. George, P.A. Shah, P.S. Shrivastav, Natural biodegradable polymers based nano-formulations for drug delivery: a review, Int. J. Pharm. 561 (2019) 244–264, https://doi.org/10.1016/j.ijpharm.2019.03.011.
[16] Y. Dong, Z. Wei, C. Xue, Recent advances in carrageenan-based delivery systems for bioactive ingredients: a review, Trends Food Sci. Technol. 112 (2021) 348–361, https://doi.org/10.1016/j.tifs.2021.04.012.
[17] N. Sarfraz, I. Khan, Plasmonic gold nanoparticles (AuNPs): properties, synthesis and their advanced energy, environmental and biomedical applications, Chem. Asian J. 16 (2021) 720–742, https://doi.org/10.1002/asia.202001202.
[18] Z. Hua, T. Yu, D. Liu, Y. Xianyu, Recent advances in gold nanoparticles-based biosensors for food safety detection, Biosens. Bioelectron. 179 (2021), https://doi.org/10.1016/j.bios.2021.113076.
[19] T. Ahmad, J. Iqbal, M.A. Bustam, M. Irfan, H.M.Anwaar Asghar, A critical review on phytosynthesis of gold nanoparticles: issues, challenges and future perspectives, J. Clean. Prod. 309 (2021) 127460, https://doi.org/10.1016/j.jclepro.2021.127460.
[20] N. González-Ballesteros, M.D. Torres, N. Flórez-Fernández, L. Diego-González, R. Simón-Vázquez, M.C. Rodríguez-Argüelles, H. Domínguez, Eco-friendly extraction of *Mastocarpus stellatus* carrageenan for the synthesis of gold nanoparticles with improved biological activity, Int. J. Biol. Macromol. 183 (2021) 1436–1449, https://doi.org/10.1016/j.ijbiomac.2021.05.115.
[21] G. Decante, J.B. Costa, J. Silva-Correia, M.N. Collins, R.L. Reis, J.M. Oliveira, Engineering bioinks for 3D bioprinting, Biofabrication 13 (2021), https://doi.org/10.1088/1758-5090/abec2c.
[22] I. Diañez, C. Gallegos, E. Brito-de la Fuente, I. Martínez, C. Valencia, M.C. Sánchez, M.J. Diaz, J.M. Franco, 3D printing in situ gelification of κ-carrageenan solutions: effect of printing variables on the rheological response, Food Hydrocoll. 87 (2019) 321–330, https://doi.org/10.1016/j.foodhyd.2018.08.010.
[23] A. Bianchi, V. Sanz, H. Domínguez, M.D. Torres, Valorisation of the industrial hybrid carrageenan extraction wastes using eco-friendly treatments, Food Hydrocoll. 122 (2022), 107070, https://doi.org/10.1016/j.foodhyd.2021.107070.
[24] G. Azevedo, M.D. Torres, I. Sousa-Pinto, L. Hilliou, Effect of pre-extraction alkali treatment on the chemical structure and gelling properties of extracted hybrid carrageenan from *Chondrus crispus* and *Ahnfeltiopsis devoniensis*, Food Hydrocoll. 50 (2015) 150–158, https://doi.org/10.1016/j.foodhyd.2015.03.029.
[25] R.P. Overend, E. Chornet, J.A. Gascoigne, Fractionation of lignocellulosics by steam-aqueous pretreatments, Philos. Trans. R. Soc. London. Ser. A, Math. Phys. Sci. 321 (1987) 523–536, https://doi.org/10.1098/rsta.1987.0029.
[26] M.D. Torres, N. Flórez-Fernández, H. Domínguez, Chondrus crispus treated with ultrasound as a polysaccharides source with improved antitumoral potential, Carbohydr. Polym. 273 (2021), https://doi.org/10.1016/j.carbpol.2021.118588.
[27] M. Barral-Martínez, N. Flórez-Fernández, H. Domínguez, M.D. Torres, Tailoring hybrid carrageenans from *Mastocarpus stellatus* red seaweed using microwave hydrodiffusion and gravity, Carbohydr. Polym. 248 (2020), 116830, https://doi.org/10.1016/j.carbpol.2020.116830.
[28] S.O. Lourenço, E. Barbarino, J.C. De-Paula, L.O.D.S. Pereira, U.M. Lanfer Marquez, Amino acid composition, protein content and calculation of nitrogen-to-protein conversion factors for 19 tropical seaweeds, Phycol. Res. 50 (2002) 233–241, https://doi.org/10.1046/j.1440-1835.2002.00278.x.
[29] E. Gómez-Ordóñez, E. Alonso, P. Rupérez, A simple ion chromatography method for inorganic anion analysis in edible seaweeds, Talanta 82 (2010) 1313–1317, https://doi.org/10.1016/j.talanta.2010.06.062.
[30] K.S. Dodgson, Determination of inorganic sulphate in studies on the enzymic and non-enzymic hydrolysis of carbohydrate and other sulphate esters, Biochem. J. 78 (1961) 312.
[31] J.R. Wiśniewski, M. Mann, Consecutive proteolytic digestion in an enzyme reactor increases depth of proteomic and phosphoproteomic analysis, Anal. Chem. 84 (2012) 2631–2637, https://doi.org/10.1021/ac300006b.
[32] I.F.F. Benzie, J.J. Strain, The ferric reducing ability of plasma (FRAP) as a measure of "antioxidant power": the FRAP assay, Anal. Biochem. 239 (1996) 70–76.
[33] R. Re, N. Pellegrini, A. Proteggente, A. Pannala, M. Yang, C. Rice-Evans, Antioxidant activity applying an improved ABTS radical cation decolorization assay, Free Radic. Biol. Med. 26 (1999) 1231–1237.
[34] A. von Gadow, E. Joubert, C.F. Hansmann, Comparison of the antioxidant activity of rooibos tea (*Aspalathus linearis*) with green, oolong and black teas, Food Chem. 60 (1997) 73–77, https://doi.org/10.1080/09637480500398835.
[35] R. Pangestuti, A.T. Getachew, E.A. Siahaan, B.S. Chun, Characterization of functional materials derived from tropical red seaweed *Hypnea musciformis* produced by subcritical water extraction systems, J. Appl. Phycol. 31 (2019) 2517–2528, https://doi.org/10.1007/s10811-019-1754-9.
[36] S. Machmudah, S.Winardi Widiyastuti, H. Wahyudiono, M.Goto Kanda, Sub-and supercritical fluids extraction of phytochemical compounds from *Eucheuma cottonii* and *Gracilaria* sp, Chem. Eng. Trans. 56 (2017) 1291–1296, https://doi.org/10.3303/CET1756216.
[37] G. Azevedo, L. Hilliou, G. Bernardo, I. Sousa-Pinto, R.W. Adams, M. Nilsson, R. D. Villanueva, Tailoring kappa/iota-hybrid carrageenan from *Mastocarpus stellatus* with desired gel quality through pre-extraction alkali treatment, Food Hydrocoll. 31 (2013) 94–102, https://doi.org/10.1016/j.foodhyd.2012.10.010.

[38] E. Trigueros, M.T. Sanz, P. Alonso-Riaño, S. Beltrán, C. Ramos, R. Melgosa, Recovery of the protein fraction with high antioxidant activity from red seaweed industrial solid residue after agar extraction by subcritical water treatment, J. Appl. Phycol. 33 (2021) 1181–1194, https://doi.org/10.1007/s10811-020-02349-0.
[39] M. Álvarez-Viñas, N. Flórez-Fernández, M.D. Torres, H. Domínguez, Successful approaches for a red seaweed biorefinery, Mar. Drugs 17 (2019), https://doi.org/10.3390/md17110620.
[40] L. Dufossé, P. Galaup, A. Yaron, S.M. Arad, P. Blanc, K.N.C. Murthy, G. A. Ravishankar, Microorganisms and microalgae as sources of pigments for food use: a scientific oddity or an industrial reality? Trends Food Sci. Technol. 16 (2005) 389–406, https://doi.org/10.1016/j.tifs.2005.02.006.
[41] S. Sekar, M. Chandramohan, Phycobiliproteins as a commodity: trends in applied research, patents and commercialization, J. Appl. Phycol. 20 (2008) 113–136, https://doi.org/10.1007/s10811-007-9188-1.
[42] Y. Liu, L. Xu, N. Cheng, L. Lin, C. Zhang, Inhibitory effect of phycocyanin from *Spirulina platensis* on the growth of human leukemia K562 cells, J. Appl. Phycol. 12 (2000) 125–130, https://doi.org/10.1023/A:1008132210772.
[43] K.V. Sathyasaikumar, I. Swapna, P.V.B. Reddy, C.R.K. Murthy, K.R. Roy, A. Dutta Gupta, B. Senthilkumaran, P. Reddanna, Co-administration of C-phycocyanin ameliorates thioacetamide-induced hepatic encephalopathy in Wistar rats, J. Neurol. Sci. 252 (2007) 67–75, https://doi.org/10.1016/j.jns.2006.10.014.
[44] J. Riss, K. Décordé, T. Sutra, M. Delage, J.C. Baccou, N. Jouy, J.P. Brune, H. Oréal, J.P. Cristol, J.M. Rouanet, Phycobiliprotein C-phycocyanin from *Spirulina platensis* is powerfully responsible for reducing oxidative stress and NADPH oxidase expression induced by an atherogenic diet in hamsters, J. Agric. Food Chem. 55 (2007) 7962–7967, https://doi.org/10.1021/jf070529g.
[45] M. Khotimchenko, V. Tiasto, A. Kalitnik, M. Begun, R. Khotimchenko, E. Leonteva, I. Bryukhovetskiy, Y. Khotimchenko, Antitumor potential of carrageenans from marine red algae, Carbohydr. Polym. 246 (2020), 116568, https://doi.org/10.1016/j.carbpol.2020.116568.
[46] N. Flórez-Fernández, M. López-García, M.J. González-Muñoz, J.M.L. Vilariño, H. Domínguez, Ultrasound-assisted extraction of fucoidan from *Sargassum muticum*, J. Appl. Phycol. 29 (2017) 1553–1561, https://doi.org/10.1007/s10811-016-1043-9.
[47] T. Bouanati, E. Colson, S. Moins, J.C. Cabrera, I. Eeckhaut, J.M. Raquez, P. Gerbaux, Microwave-assisted depolymerization of carrageenans from *Kappaphycus alvarezii* and *Eucheuma spinosum*: controlled and green production of oligosaccharides from the algae biomass, Algal Res. 51 (2020), https://doi.org/10.1016/j.algal.2020.102054.
[48] L. Pereira, A.M. Amado, A.T. Critchley, F. van de Velde, P.J.A. Ribeiro-Claro, Identification of selected seaweed polysaccharides (phycocolloids) by vibrational spectroscopy (FTIR-ATR and FT-Raman), Food Hydrocoll. 23 (2009) 1903–1909, https://doi.org/10.1016/j.foodhyd.2008.11.014.
[49] L. Hilliou, Hybrid Carrageenans: Isolation, Chemical Structure, and Gel Properties, 1st ed., Elsevier Inc., 2014 https://doi.org/10.1016/B978-0-12-800269-8.00002-6.
[50] F. Van de Velde, Structure and function of hybrid carrageenans, Food Hydrocoll. 22 (2008) 727–734, https://doi.org/10.1016/j.foodhyd.2007.05.013.
[51] M.D. Torres, N. Flórez-Fernández, H. Domínguez, Impact of counterions on the thermo-rheological features of hybrid carrageenan systems isolated from red seaweed *Gigartina skottsbergii*, Food Hydrocoll. 84 (2018) 321–329, https://doi.org/10.1016/j.foodhyd.2018.06.020.
[52] M.C. Lefatle, M.J. John, Mechanical, rheological and viscoelastic properties of polysaccharide and protein based aerogels, in: RSC Green Chem, 2018, pp. 177–200.
[53] F. Zhu, Polysaccharide based films and coatings for food packaging: effect of added polyphenols, Food Chem. 359 (2021), 129871, https://doi.org/10.1016/j.foodchem.2021.129871.
[54] S.K. Bharti, V. Pathak, A. Arya, T. Alam, V. Rajkumar, A.K. Verma, Packaging potential of *Ipomoea batatas* and κ-carrageenan biobased composite edible film: its rheological, physicomechanical, barrier and optical characterization, J. Food Process. Preserv. 45 (2021), https://doi.org/10.1111/jfpp.15153.
[55] H.P.S. Abdul Khalil, C.K. Saurabh, Y.Y. Tye, T.K. Lai, A.M. Easa, E. Rosamah, M.R. N. Fazita, M.I. Syakir, A.S. Adnan, H.M. Fizree, N.A.S. Aprilia, A. Banerjee, Seaweed based sustainable films and composites for food and pharmaceutical applications: a review, Renew. Sust. Energ. Rev. 77 (2017) 353–362, https://doi.org/10.1016/j.rser.2017.04.025.
[56] J. BeMiller, R. Whistler, Starch Chemistry and Technology, 2009.
[57] S. David, C. Shani Levi, L. Fahoum, Y. Ungar, E.G. Meyron-Holtz, A. Shpigelman, U. Lesmes, Revisiting the carrageenan controversy: do we really understand the digestive fate and safety of carrageenan in our foods? Food Funct. 9 (2018) 1344–1352, https://doi.org/10.1039/c7fo01721a.
[58] E.R. Gasilova, G.P. Aleksandrova, B.Z. Volchek, E.N. Vlasova, V.A. Baigildin, Smart colloids containing ensembles of gold nanoparticles conjugated with κ-carrageenan, Int. J. Biol. Macromol. 137 (2019) 358–365, https://doi.org/10.1016/j.ijbiomac.2019.06.215.
[59] M.V. Lesnichaya, B.G. Sukhov, G.P. Aleksandrova, E.R. Gasilova, T.I. Vakul'skaya, S.S. Khutsishvili, A.N. Sapozhnikov, I.V. Klimenkov, B.A. Trofimov, Chiroplasmonic magnetic gold nanocomposites produced by one-step aqueous method using κ-carrageenan, Carbohydr. Polym. 175 (2017) 18–26, https://doi.org/10.1016/j.carbpol.2017.07.040.
[60] H. Wan, Z. Liu, Q. He, D. Wei, S. Mahmud, H. Liu, Bioreduction (AuIII to Au0) and stabilization of gold nanocatalyst using kappa carrageenan for degradation of azo dyes, Int. J. Biol. Macromol. 176 (2021) 282–290, https://doi.org/10.1016/j.ijbiomac.2021.02.085.
[61] N. González-Ballestero, M.D. Torres, N. Flórez-Fernández, L. Diego-González, R. Simón-Vázquez, M.C. Rodríguez-Argüelles, H. Domínguez, Eco-friendly Extraction of *Mastocarpus stellatus* Carrageenan for the Synthesis of Gold Nanoparticles With Improved Biological Activity, 2021.